ORIGINAL ARTICLE

FISHERIES OCEANOGRAPHY | WILEY

Size-selective predation effects on juvenile Chinook salmon cohort survival off Central California evaluated with an individual-based model

Kelly Vasbinder[1] | Jerome Fiechter[1] | Jarrod A. Santora[2,3] |
James J. Anderson[4] | Nate Mantua[2] | Steve T. Lindley[2] | David D. Huff[5] |
Brian K. Wells[2,5,6]

[1]Department of Ocean Sciences, University of California at Santa Cruz, Santa Cruz, California, USA

[2]Fisheries Ecology Division, Southwest Fisheries Science Center, National Marine Fisheries Service, Santa Cruz, California, USA

[3]Department of Applied Math, University of California, Santa Cruz, California, USA

[4]School of Aquatic and Fishery Sciences, University of Washington, Seattle, Washington, USA

[5]Fish Ecology Division, Northwest Fisheries Science Center, National Marine Fisheries Service, National Oceanic and Atmospheric Administration, Newport, Oregon, USA

[6]College of Earth, Ocean, and Atmospheric Sciences, Oregon State University, Corvallis, Oregon, USA

Correspondence
Kelly Vasbinder, Department of Ocean Sciences, University of California at Santa Cruz, Santa Cruz, CA, USA.
Email: kvasbind@ucsc.edu

Abstract

Variation in the recruitment of salmon is often found to be correlated with marine climate indices, but mechanisms behind environment–recruitment relationships remain unclear and correlations often break down over time. We used an ecosystem modeling approach to explore bottom-up and top-down mechanisms linking a variable environment to salmon recruitment variations. Our ecosystem model incorporates a regional ocean circulation submodel for hydrodynamics, a nutrient-phytoplankton-zooplankton submodel for producing planktonic prey fields, and an individual-based model (IBM) representing juvenile Chinook salmon (*Oncorhynchus tshawytscha*), combined with observations of foraging distributions and diet of a seabird predator. The salmon IBM consists of modules, including a juvenile salmon growth module based on temperature and salmon–prey availability, a behavior-based movement module, and a juvenile salmon predation mortality module based on juvenile salmon size distribution and predator–prey interaction probability. Seabird–salmon interactions depend on spatial overlap and juvenile salmon size, whereby salmon that grow past the size range of the prey distribution of the predator will escape predation. We used a 21-year historical simulation to explore interannual variability in juvenile Chinook salmon growth and predation-mediated survival under a range of ocean conditions for sized-based mortality scenarios. We based a series of increasingly complex predation scenarios on seabird observational data to explore variability in predation mortality on juvenile Chinook salmon. We initially included information about the predator spatial distribution, then added population size, and finally the predator's diet percentage made up of juvenile salmon. Model agreement improves with added predator complexity, especially during periods when predator abundance is high. Overall, our model found that when the fraction of juvenile salmon in seabird diet increased relative to alternate prey (e.g., Northern anchovy *Engraulis mordax*, and juvenile rockfish *Sebastes* spp.), there was a concomitant decrease in salmon cohort survival during their first year at sea.

1 | INTRODUCTION

Chinook salmon, *Oncorhynchus tshawytscha*, is an anadromous species that, in its North American range, spawn in rivers ranging from Alaska to Central California (Groot & Margulis, 1991; Weitkamp, 2010). Fall-run Chinook salmon in California's Central Valley typically return from the ocean to their natal rivers after one to four winters at sea to spawn, and "ocean type" smolts migrate to sea a few months after hatching (Fiechter et al., 2015; Friedman et al., 2019; Healey, 1991; Myers et al., 1998; Trudel et al., 2007, 2012). For fall-run Chinook salmon emigrating from California's Central Valley, this transformation to the smolt stage and subsequent ocean entry occurs in the spring (Friedman et al., 2019; Myers et al., 1998; Wells et al., 2017).

Early marine survival and growth of juvenile Central Valley Chinook salmon are correlated with the timing and strength of upwelling (Fiechter et al., 2015, Henderson et al., 2019). Along the Central California coast, strong, southward winds lead to persistent seasonal upwelling from the spring transition (typically March) through the summer and into early fall, while more intermittent northward winds typically cause coastal downwelling in the late fall and winter (Largier et al., 2006). Point Reyes, at the northern end of the Gulf of the Farallones (GoF), is an important upwelling center, while in the lee of Point Reyes, a zone of less dense, warmer water is typically found in an upwelling shadow that can act as a retention area for forage (Graham & Largier, 1997; Graham et al., 1992; Santora et al., 2012; Wing et al., 1998). Coastal upwelling is inherently variable over a wide range of spatial and temporal scales, meaning that juvenile Central Valley Chinook salmon typically encounter a complex and dynamic environment upon entering the ocean in the GoF (Fiechter et al., 2015; Wells et al., 2012, 2017).

Early marine growth of juvenile salmon is a key determinant of marine survival and impacts brood year strength in Pacific salmon species (Beamish et al., 2004; Duffy & Beauchamp, 2011; Pearcy, 1992). The transitional period for Chinook salmon directly following ocean entry has the potential for highly variable growth and associated size-selective mortality and is a critical period for determining cohort survival (Beamish & Mahnken, 2001; MacFarlane, 2010; Wells et al., 2016; Woodson et al., 2013). Previous modeling studies have used a ROMS-NEMURO framework to predict macro-zooplankton and temperature dynamics as inputs to a juvenile salmon growth model under a "bottom-up" ecosystem modeling framework (Fiechter et al., 2015; Wells et al., 2017), and those results support the idea that bottom-up forces are important for early marine survival of Chinook salmon. While juveniles experience their greatest rate of growth during this period, growth and condition are dependent on environmental variables such as the onset of upwelling (Fiechter et al., 2015), food availability (MacFarlane, 2010; Sabal et al., 2020; Wells et al., 2012,

2016), and temperature-dependent effects on bioenergetics (Daly & Brodeur, 2015). In this region, krill are indicative of the juvenile salmon forage base (MacFarlane & Norton, 2002, Wells et al., 2012, 2023), and the condition of juvenile Chinook in the GoF is associated with the availability and spatial distribution of krill (Fiechter et al., 2015; Henderson et al., 2019; Wells et al., 2012). For instance, above-average years for juvenile growth and survival at sea have been linked to early season upwelling driving high krill abundances and good prey retention in nearshore waters where juvenile Chinook salmon enter the ocean (Fiechter et al., 2015; Wells et al., 2012, 2016, 2020). In contrast, anomalous ocean conditions concomitant with weak or late upwelling can result in warmer ocean temperatures, less spatial heterogeneity of the environment (e.g., reduced upwelling shadows, eddies, and fronts), and reduced prey concentration and availability at the time of ocean entry, each of which has been associated with stock collapses and low survival years for Central California Chinook salmon (Graham & Largier, 1997; Lindley et al., 2009; MacFarlane, 2010; Sabal et al., 2020; Wells et al., 2012, 2016; Wing et al., 1998; Woodson & Litvin, 2015). While juvenile Chinook salmon growth potential has also been shown to correlate with upwelling timing, de-trended sea-level anomalies, and the strength of cross-shore currents, the ability of these environmental drivers and resultant krill abundance to explain survival is stronger for low survival years (Henderson et al., 2019). This supports an argument that when environmental conditions are not ideal, the environment has an indirect control on survival potentially through size-selective mortality, but when conditions are favorable and prey is abundant, environmental drivers explain less of the observed early marine Chinook salmon survival variations (Wells et al., 2017; Woodson et al., 2013).

Critical size, the notion that juveniles must reach a certain size to maintain metabolic balance and escape predation, and critical period, the notion that this critical size must be reached during a certain time window to escape predation, have both been suggested to be important for juvenile salmon species (Beamish & Mahnken, 2001; Hjort, 1914). Vulnerability to predation depends on the ability of prey to gain refuge from predators. Prey can be thought of as belonging to a vulnerable pool to which predators have access or an invulnerable pool that predators cannot access (Walters & Juanes, 1993). This invulnerable pool could gain refuge through a lack of spatial and temporal overlap with predators, through prey-switching by predators, or by outgrowing the gape range of the predators; the latter is known as the size-refuge hypothesis for juvenile salmon, whereby more rapid growth reduces vulnerability (Walters & Juanes, 1993; Willette, 2001; Willette et al., 2001). Here, we examine the variability of predation mortality on juvenile Chinook salmon off Central California through a series of increasingly complex model scenarios informed by empirical observations. These scenarios start with a size-limited mortality case, in which interactions are controlled by (1) juvenile salmon size, which

depends on size at ocean entry and early marine growth rates, and extensions that include (2) spatial overlap with gape-limited predators, (3) predator population size, and (4) predator diet. This approach allows us to explore the ability of juvenile salmon to escape predation by growing out of the preferred prey size range, finding spatial refuge outside the predator's foraging distribution, or reprieve from predation due to alternate prey availability.

2 | METHODS

2.1 | Ecosystem modeling framework

The ecosystem modeling framework is based on Fiechter et al. (2015) and includes a regional ocean circulation model (ROMS), a nutrient-phytoplankton-zooplankton (NPZ) model, and an individual-based model (IBM) for juvenile Chinook salmon. The main additions of the modeling framework used here (over that used by Fiechter et al., 2015) are (1) an increase in spatial resolution to better-resolve local upwelling variability, (2) an NPZ model specifically parameterized to represent the dominant krill species (*Euphausia pacifica*) off California (Fiechter et al., 2020), and (3) the addition of a salmon mortality component including size- and distribution-based prey–predator interactions. A brief overview of the different submodels is given below, and additional details can be found in Fiechter et al. (2015), Henderson et al. (2019), and Fiechter et al. (2020).

2.2 | Ocean circulation and ecosystem submodels

The ocean circulation model is an implementation of the Regional Ocean Modeling System (ROMS) for the Central California Current region (32–44°N) at 1/30° resolution (Fiechter et al., 2018, 2020). To improve the representation of regional circulation patterns and variability, the 1/30° ROMS domain is nested within a physical reanalysis of the broader California Current System at 1/10° (Neveu et al., 2016). The NPZ model, NEMUCSC, is a customized version of the North Pacific Ecosystem Model for Understanding Regional Oceanography (NEMURO) (Kishi et al., 2007) specifically parameterized for the California Current (Fiechter et al., 2018, 2020). NEMUCSC accounts for biogeochemical interaction through macro-nutrients, phytoplankton, zooplankton, and detritus pools. The planktonic functional groups include nanoplankton and diatoms as primary producers and micro, meso, and predatory zooplankton groups as grazers. The predatory zooplankton group is further parameterized to represent the growth rates and diet preferences of the dominant krill species in the Central California Current region, *E. pacifica* (Brinton, 1962; Fiechter et al., 2020; Santora et al., 2012). The krill distributions simulated by ROMS-NEMUCSC have been evaluated against in situ data and generally reproduce the spatial and temporal patterns of observed krill aggregation regions in the Central California Current (Fiechter et al., 2020, Santora et al., 2012, for distributions). Governing equations and parameterization values for the growth,

mortality, and mixing for the predatory zooplankton group can be found in the supplement of Fiechter et al., 2020. Specific parameter values used in NEMUCSC to represent krill and other planktonic functional groups can be found in the supplementary material of Fiechter et al., 2018 and 2021.

2.3 | Juvenile salmon and predation mortality formulation

Individual-based models, also referred to as agent-based models, track individual agents through space and time in the model domain. The IBM for juvenile Chinook salmon consists of a series of modules representing growth, behavioral movement, and mortality (Fiechter et al., 2015). The IBM is rooted in the DEBkiss framework, an approach that models an individual's traits based on a dynamic energy budget tracking mass fluxes throughout the organism's lifespan (Jager et al., 2013). The flux equations for our IBM can be found in the supplementary material of Fiechter et al., 2015. Growth is calculated via metabolic equations using the temperature and krill fields from the ROMS and NEMUCSC models. ROMS supplies upwelling dynamics to NEMUCSC and temperature fields to the IBM, and NEMUCSC provides prey fields to the IBM (Fiechter et al., 2015). To improve computational efficiency, the IBM is run offline in the sense that it reads in precalculated daily physical and prey fields from ROMS-NEMUCSC and uses them in a series of metabolic equations to calculate juvenile Chinook salmon growth. The resulting simulated growth curves show comparable size ranges with observational data for fall subyearling juvenile Chinook salmon (MacFarlane, 2010; Trudel et al., 2007).

The juvenile Chinook salmon behavioral movement in the model is based on an area-restricted search algorithm where salmon individuals move toward the neighboring model grid cell with the highest krill concentrations (Fiechter et al., 2018; Watkins & Rose, 2013). To represent behavioral uncertainty, a random deviation normally distributed between −45° and 45° is added to the swimming direction each time movement is updated. The resulting distribution of juvenile salmon shows a similar spatial mean to survey data and presence/absence data (Figure 2 in Henderson et al., 2019, fig. 7f in Santora et al., 2012).

In the present study, we detail the addition of a salmon predation mortality component to the IBM, which provides the capability to diagnose factors most related to survival and recruitment. This new mortality component is parameterized to include predation from a central-place feeder, but the framework has the flexibility to add other types of predators (e.g., migratory species) in the future. Here, the central-place predator represents common murre (*Uria aalge*), whose largest breeding colony off the US west coast is located in the GoF. Predation mortality is calculated through a size-dependent approach using a prey size distribution and interaction probability. The consequences of interactions between juvenile salmon and the central-place predator depend on the size of juvenile salmon, whereby individuals outgrowing the size of the prey distribution of the central-place feeder will escape predation.

2.3.1 | Generating a prey size distribution for common murre

To generate a prey size distribution for the predator, a normal distribution was reconstructed from annual diet observations of adult common murre individuals returning from foraging trips at the Southeast Farallon Island (Santora, Rogers, et al., 2021; Warzybok et al., 2018; Wells et al., 2017). We calculated a combined weighted variance for the entire survey period for each prey species using the R package *fishmethods* (Nelson, 2019). This combined variance was used to calculate the mean and standard deviation of prey sizes. A simulated normal distribution was generated using the *stats* package. Then all prey species were combined using a mixed distribution to generate a 95% range that included all prey using the *Kscorrect* package (Bolar, 2019; Wang & Novack-Gottshall, 2016). The simulated prey distributions for our central place predator yielded a distribution with a mean of 104 mm and a standard deviation of 15.0 mm (Figure 1b).

2.3.2 | Predation mortality formulation and parameterization

The predation mortality rate was calculated by combining the probability of predator–prey interaction with the probability of prey falling within the predation size range during this interaction using the gape-limited mortality framework of Anderson (2019):

$$\mu_{i,t} = \lambda \frac{1 - \phi(x_{i,t})}{\phi\left(\frac{m}{s}\right)} \tag{1}$$

where, predation mortality, μ, for model individual i at time step t combines a term representing a daily encounter rate between predator and prey, λ, with a term representing the probability of prey being within a predator's gape range. ϕ, a standardized cumulative normal distribution, is calculated for prey in the numerator and predator in the denominator, in which it becomes a scaling factor that is near unity. $x_{i,t}$ represents the prey and is calculated using the prey size ($l_{i,t}$) normalized by the mean (m) and standard deviation (s) of the predator gape range (Anderson, 2019):

$$x_{i,t} = \frac{l_{i,t} - m}{s} \tag{Eq2}$$

This predation model was coded in Fortran90 using the Cumnor function (William, 1969, 1993).

λ is a tunable parameter, calibrated here to yield predation mortality falling within the estimated range of juvenile salmon survival from Friedman et al. (2019) in which background survival to the end of year one without predation is estimated at approximately 25% and decreases to roughly 3% with predation. Therefore, total mortality in the IBM is tuned for a constant natural mortality rate yielding a 25%
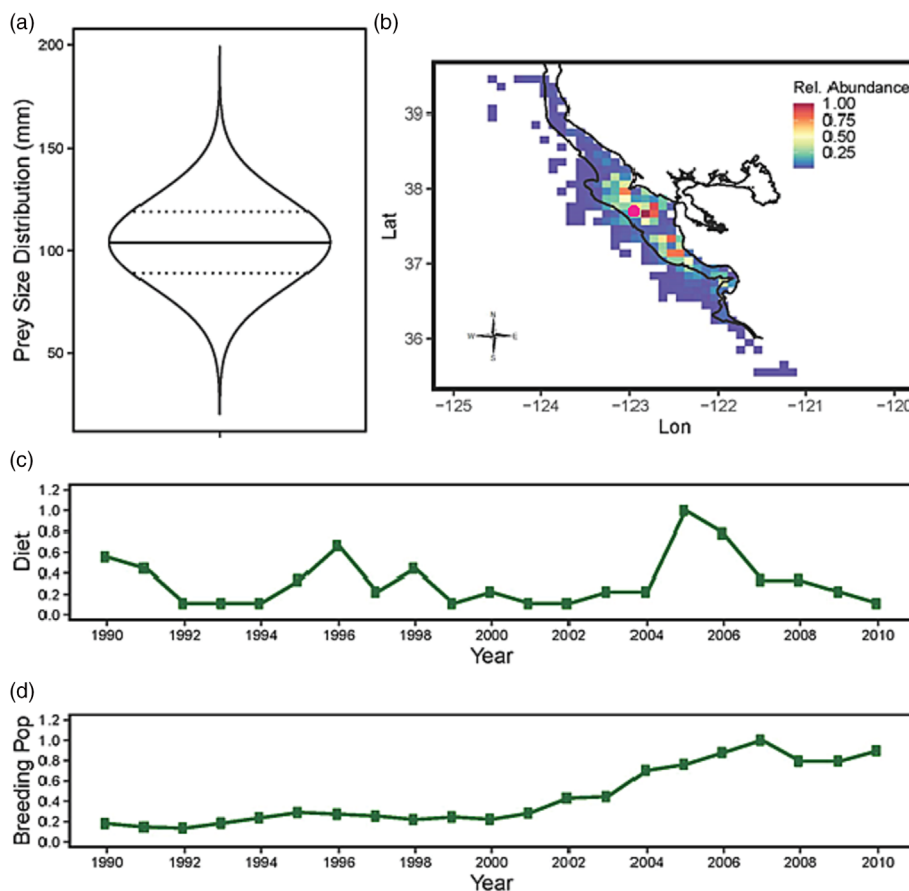

FIGURE 1 Predator attributes for size-based mortality based on common murre. (a) Probability density for the preferred size range of prey with lines indicating the values provided to the mortality submodule. The solid line represents a mean of 104 mm and the dotted lines represent ±1 standard deviation of 15.0 mm. (b) Normalized relative abundance and spatial distribution of common murre in the greater gulf of the Farallones. The Southeast Farallon Island station is denoted by a magenta point. (c) Time series of proportion of common murre diet made up of salmon normalized so that the maximum value is one. (d) Time series of the relative size of common murre breeding population normalized so that the maximum value is one.

—WILEY |

annual survival fraction and a daily predation mortality rate explicitly associated with common murre defined as

$$\lambda = f * \alpha \tag{3}$$

where f is a scaling coefficient ranging between 0 and 1 and accounting for additional attributes of the predator population (e.g., spatial distribution, abundance, and diet), and α is a tuning parameter used to match expected survival. Predation mortality (μ) is tuned using the α parameter so that under full predation (i.e., $f = 1$), total daily mortality (predation mortality + natural mortality) cumulated over the year yields an annual survival fraction of 3%. In the absence of explicit predation from common murre (i.e., $\mu = 0$), we recover the annual survival rate of 25% associated with background natural mortality.

Parameter values are listed in Table 1. α was tuned to yield a predation mortality over 245 days at sea (May 1–December 31) of 2.171 using a distribution of prey sizes for the predator, as the distributions in the mortality Equation (1). After the observed distribution of common murre relative abundance was added to the IBM, α was re-tuned for the remaining scenarios so that we recovered a survival fraction of 3% by the end of the year under maximum predation pressure (i.e., $f = 1$). Predation mortality is updated at each time step (6 h) in the IBM.

2.4 | Predation scenarios

Predation was included as four levels of increasing complexity (Table 1). Predation scenario development was approached with the MICE framework in mind (Plagányi et al., 2014). MICE models, or

TABLE 1 Predation scenarios.

Scenario	f value	α
1 - size-dependent mortality only	1	0.051
2 - size-dependent mortality and spatially-varying predator distribution	0 if no predator overlap 1 if predator overlap	0.57
3 - size-dependent mortality, spatially-varying predator distribution, and temporally-varying predator abundance	Predator abundance per year/maximum abundance	0.57
4 - size-dependent mortality, spatially-varying predator distribution, temporally-varying predator abundance, and salmon fraction in predator's diet	((predator abundance per year)/(maximum abundance)) × (normalized percentage of diet comprised of salmon)	0.57

Note: The f-value represents a scaling coefficient that accounts for attributes of the predator population (e.g., spatial distribution, abundance, and diet), and λ is a tunable parameter that represents the probability of interaction between predator and prey.

Models of Intermediate Complexity for Ecosystem assessments, are a type of minimum realism model that include just enough information on the ecosystem to address a specific question or investigate a specific species (Plagányi et al., 2014; Punt & Butterworth, 1995). The four scenarios for predation included in this study build from the simplest to most complex representations of predator–prey interactions. This approach allows the driver effects to be examined both independently and synergistically as drivers are added one at a time to the model. By starting with size-based mortality only and building up to a model that includes information about the predator spatial distribution, breeding population abundance, and diet composition, we can tease apart the impacts of these drivers on the predation mortality and survival of juvenile Chinook salmon during their first few months at sea.

The first and lowest complexity scenario represents predation mortality as a function of only the probability of juvenile salmon outgrowing the predator's preferred prey size distribution. The second adds the spatial overlap between predator and juvenile salmon (i.e., $f = 0$ if no predator is present in the grid cell and $f = 1$ if a predator is present in the grid cell). The third and fourth scenarios add complexity by setting f equal to a scalar between 0 and 1, representing the effects of predator abundance (Scenario 3) or predator abundance and the percent salmon in predator's diet (Scenario 4). In the third scenario, f was set to a weighted abundance of the predator, whereby common murre abundance was scaled by its maximum value over the 21-year simulation to generate a normalized abundance index between 0 and 1 for each year. In the fourth scenario, f was set to a multiplicative scalar combining diet and abundance (Table 1). Spatial variability in predation mortality was included in the IBM by scaling the predation mortality in each cell of the model domain by the observed mean relative abundance of common murre present in that cell regardless of the scaling used for f. The predator distribution shows two distinct areas of high predator abundance in the GoF region and typically decreasing predator presence close to the coast and offshore. (Figure 1). The predator population abundance increases significantly after 2000, reaching a maximum in 2007, while the percentage of salmon in predator's diet was highest in 1995 and 2005 and decreased in more recent years (Figure 1). Thus, years of high common murre abundance do not always coincide with years of a high percentage of salmon in their diet.

2.5 | Analysis of predation scenarios

The IBM tracks fish as "super-individuals," where each super-individual represents one million individual fish (all with identical attributes). These one million individuals are referred to as the "worth" of the super-individual. This super-individual and worth approach allows the number of individuals released in the model to be scaled to observed abundance levels while maintaining a computationally tractable number of super-individuals. As mortality is experienced, the worth of the super-individual decreases. Survival is tracked through the worth of each super-individual after predation is experienced. In

this study, growth, behavioral movement, predation mortality, and worth were calculated using a 6-hour time step in the IBM and output at a daily frequency. Juvenile salmon enter the model domain at 87.1 mm (7.4 g) at the mouth of San Francisco Bay (Fiechter et al., 2015; MacFarlane, 2010) and are tracked using 100 super-individuals released each day over a 2-month ocean entry period spanning April and May, for a total of 6100 super-individuals over the entire release period. The analysis of the simulations focuses on fish that entered the ocean during May at the peak of outmigration (Brandes & McLain, 2001) and is restricted to coastal areas inshore of the 200-m isobath where juvenile salmon are typically found (Hassrick et al., 2016). For the first 90 days following ocean entry, predation mortality was calculated from decreases in worth and averaged over all individuals to produce a heatmap of predation mortality by days since ocean entry and year. Predation mortality was subsequently averaged to produce a single value for each day and each year. The change in total worth of the population was calculated to create a time series of annual survival indices.

To assess the benefits of the increasingly complex predation scenarios, Taylor diagrams (Taylor, 2001) were prepared to show the root-mean-squared differences (RMSD) model-data correlations, and ratios of simulated to observed standard deviations. In a Taylor diagram, the ratio of simulated to observed standard deviation is represented as the radial distance and model-data correlation as the azimuthal angle. Geometrically, the RMSD (normalized by the observed standard deviation) is represented by the distance between any model data point and the point (1,1), representing perfect agreement with the observations (correlation of 1 and identical standard deviation).
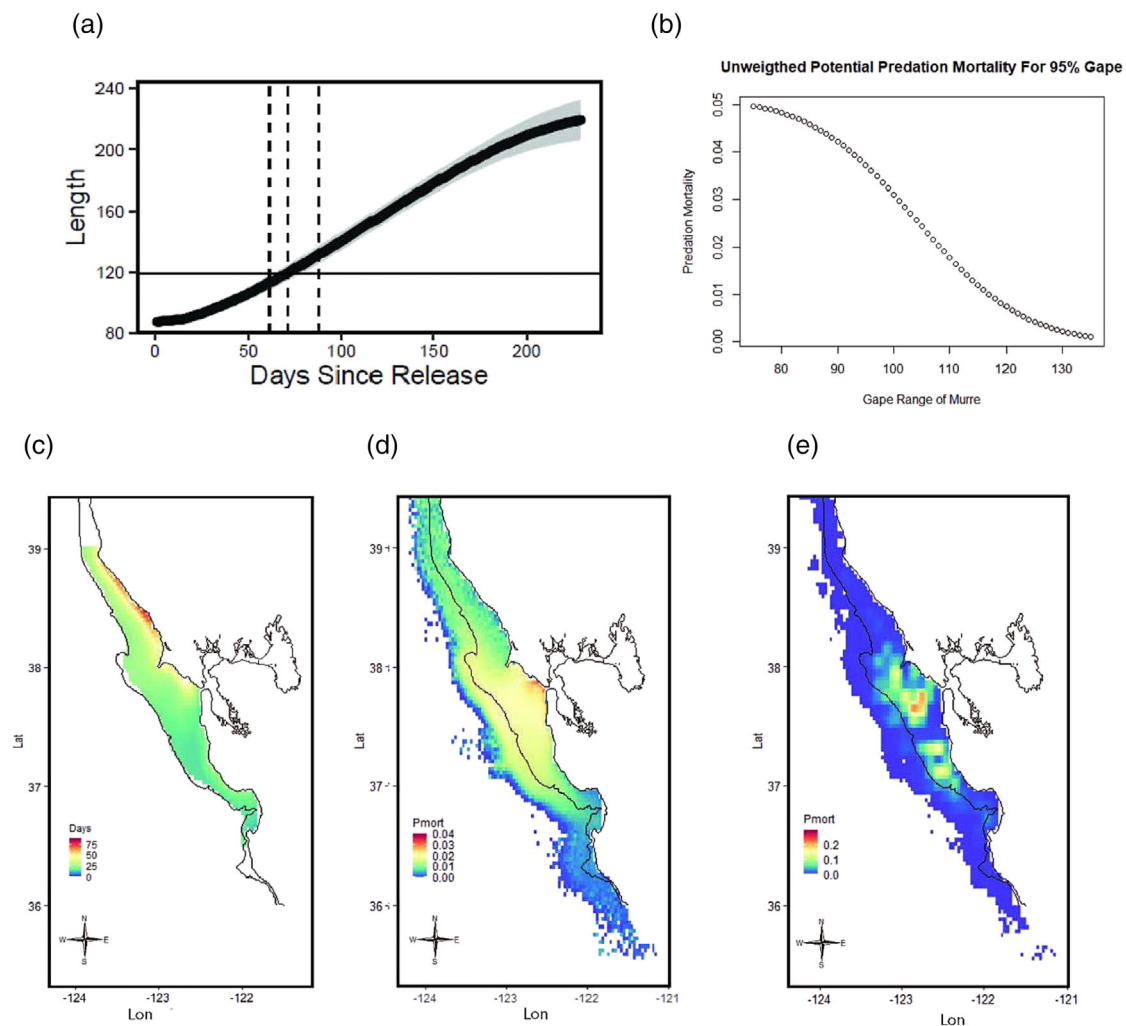

FIGURE 2 Simulated size at age and spatial mortality patterns for scenarios including only size-based mortality and spatial predator distribution. (a) Length at age for the size-dependent mortality-only scenario (scenario 1, $f = 1$) with dashed lines indicating date of escape for the minimum, maximum, and mean lengths. (b) Potential predation mortality over the range of the common murre prey size distribution. (c) Simulated days to reach 119 mm (mean of common murre simulated prey size distribution plus one standard deviation) through the main range of the study area. (d) Map of average predation mortality over the first 90 days for the size-dependent-mortality-only scenario (Scenario 1 in Table 1). (e) Map of average predation mortality over the first 90 days at sea for the size-dependent mortality and predator spatial distribution scenario (Scenario 2 in Table 1). Solid lines in Panels (d) and (e) represent 200-m isobath.

3 | RESULTS

3.1 | Size-based predation mortality with and without a predator distribution field

In our simulations, juvenile Chinook salmon are specified to enter the ocean within the expected prey size window of common murre, meaning they are immediately vulnerable to predation. Our model predicts that juvenile salmon typically grow out of the most common murre prey size range 2 to 3 months after ocean entry, with juveniles from years of faster growth able to escape murre predation almost a month before juveniles from years of slower growth (Figure 2a). The potential predation mortality over the range of the common murre prey-size distribution (Figure 2b) decreases as the prey size increases, confirming that increased growth of prey toward the upper limit of the murre prey-size range leads to decreased predation mortality. Thus, a purely size based mortality model with no additional information included on the predator allows salmon to escape predation by growing past the range of prey sizes consumed by the predator. Growth potential predicted from NEMUCSC and ROMS can be used to assess how long it would take a juvenile salmon to reach the mean

size distribution plus one standard deviation, 119 mm, in days from entry under a fully size-dependent scenario (Figure 2c).

In a purely size based predation scenario (1), juvenile salmon growth in the GoF shows relatively important interannual variability between good and poor growth years, with a mean size of 219.35 mm (±13.1 mm standard deviation, with a range from 196.31 mm to 237.65 mm) at the end of their first year at sea (Figure 2a). In Scenario 1, predation mortality peaks nearest the point of ocean entry and gradually declines with distance away from this location. In Scenario 2, which includes predator distribution, predation mortality peaks farther offshore but still within the GoF in the areas where predator densities were specified to peak. When no predator distribution is imposed (Scenario 1), spatially-varying predation risks are based solely on the ability of juveniles in each grid cell to grow out of the size range vulnerable to predation (Figure 2c,d). When a predator distribution is imposed (Scenario 2), the model predicts that the predation mortality field is strongly spatially correlated with the predator density field (Figure 2e). Scenario 2 leads to two primary locations of higher predation, one in the northern GoF near nesting areas of common murre and the other in a more southern location. Predation mortality is very low or zero where predator densities are specified to be low or zero, regardless of juvenile salmon size.
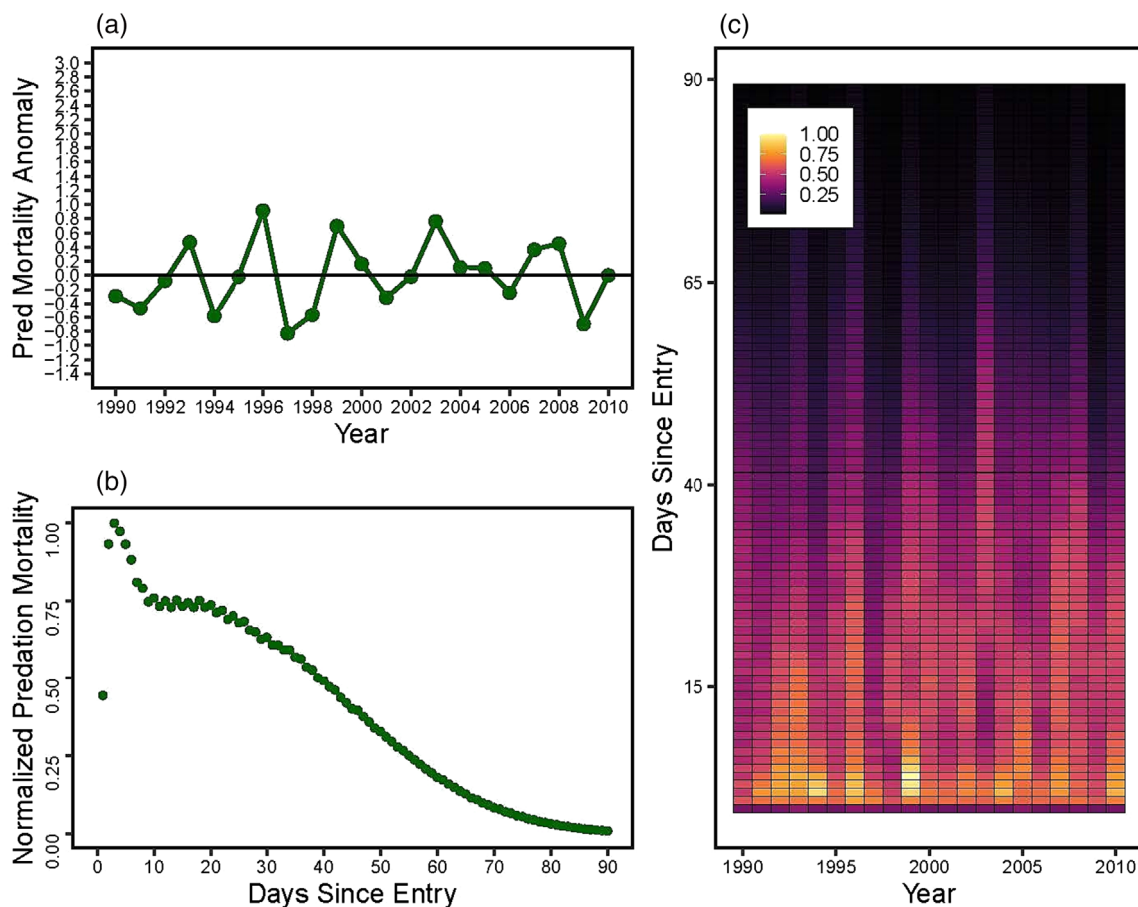

FIGURE 3 Simulated cumulative predation mortality from Scenario 2. (a) Anomaly from mean cumulative predation mortality during the first 90 days since entry. (b) Mean daily predation mortality rate averaged over all years as a function of days since entry and normalized so that the maximum value is one. (c) Normalized daily predation mortality rate by days since ocean entry for each year.

3.2 | Size-based mortality modulated by predator distribution, population, and diet

For the more realistic Scenarios 2, 3, and 4, predation mortality for juvenile salmon is greatest within the first several weeks following ocean entry and decreases steadily with increasing time spent in the ocean. In Scenario 1 where only size-based mortality is considered, the potential predation decreases as the prey outgrows the predator's prey distribution size (Figure 2b). In Scenario 2 where predator distribution is added to size-based mortality, predation by age starts low in the first several days, reaches a peak before the end of the first week as fish migrated into areas of higher predator density, then steadily decreases for the remainder of the first 90 days similar to Scenario 1, as fish outgrow the predator gape (Figure 3).

Across years, predation mortality for Scenario 2 (Figure 3) was highest in 1996 and 2003, and lowest in 1997, 1998, and 2009. Predation mortality generally exhibited a large amount of interannual variability and no significant trend over the 21-year period, reflecting bottom-up driven variations in early marine juvenile salmon growth rates.

Predation was consistently high in the first month after ocean entry across all years. In the first few days after ocean entry, higher predation occurred in 1994, 1996, and 1999, so even though 1994 and 1999 are not the highest overall predation years, higher predation pressure on juvenile salmon occurred soon after ocean entry during these years.

For Scenario 3 (Figure 4), time-varying predation mortality is dominated by the specified time-varying predator population size, and interannual variability associated with juvenile salmon growth rate variations featured in the results from Scenario 2 is largely overshadowed. Scenario 3 predation mortality showed a steadily increasing trend associated with the increase in the predator population, peaking between 2005–2008 and 2010 when predator abundance was highest. Predation in the earliest days after ocean entry was also highest between the years 2003 and 2010, again when predator abundance was highest.

For Scenario 4 (Figure 5), the substantial increase in predation mortality predicted under Scenario 3 (following 2000 associated with increasing predator abundance) is strongly modulated by adding the time-varying common murre diet composition. While predation mortality still peaks in 2006 and 2007, the low percentage of salmon in
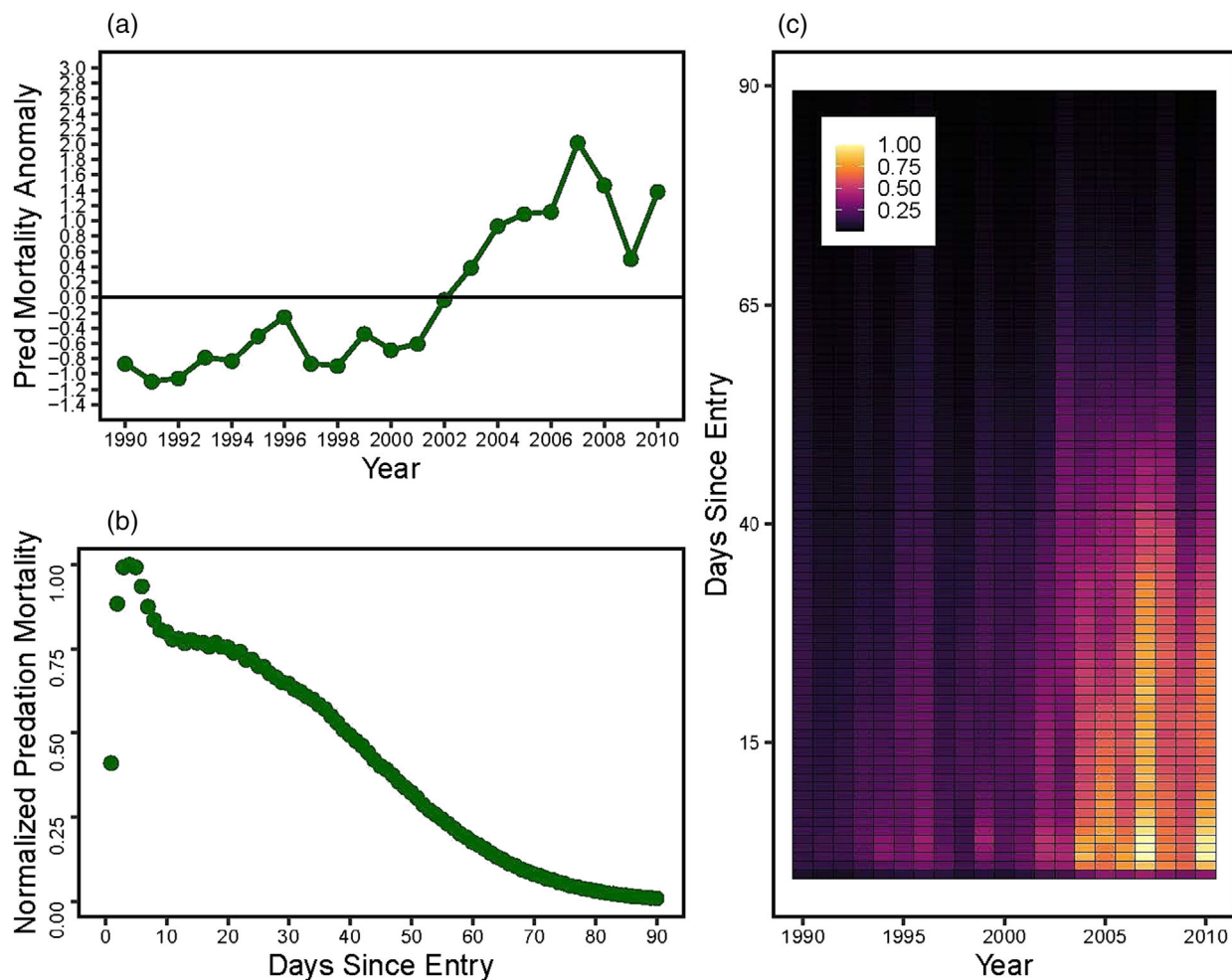

FIGURE 4 Simulated cumulative predation mortality from Scenario 3. (a) Anomaly from mean cumulative predation mortality during the first 90 days since entry. (b) Mean daily predation mortality rate averaged over all years as a function of days since entry and normalized so that the maximum value is one. (c) Normalized daily predation mortality rate by days since ocean entry for each year.

the predator diets from 2007 to 2010 greatly reduced predation mortality during these years compared with model predictions under Scenario 3. Scenario 4 predation directly following ocean entry is highest from 2005 to 2007, narrowing the range of the early ocean entry predation experienced by juvenile salmon in Scenario 3 (Figures 4c and 5c). Scenarios 2 (map only), 3 (abundance), and 4 (abundance and diet) bring the model incrementally closer to the observations of the system, as shown by the Taylor diagrams in Figure 6.

4 | DISCUSSION

4.1 | Model outcomes and considerations

We have expanded salmon IBM applications of Fiechter et al. (2015) and Henderson et al. (2019) by adding a spatially and temporally explicit predation mortality component that also includes time-varying information about predator diets. Namely, we evaluate four progressively complex model scenarios, including (1) a size-based control simulation and three additional simulations, which added incrementally (2) a static but spatially varying predator distribution, (3) a time-varying predator

abundance, and (4) time-varying predator diets. Including a spatially varying predator distribution layer resulted in no trend in the survival of juvenile Chinook salmon during their early ocean residence. The static predator distribution layer simply induces spatially and temporally concentrated areas of high mortality because of the interaction between the static predator distribution and dynamic early marine size and spatial distribution of juvenile Chinook salmon. Any temporal trend in survival brought on by the local environmentally mediated growth (i.e., simulated krill availability and surface temperature) was undiagnosed. The increasing abundance of common murre included in Scenario 3 led to a substantial negative trend in Chinook salmon early marine survival (Figure 4). Interestingly, when we included common murre proportional diet data in Scenario 4, the negative Chinook salmon survival rate trend resulting from the model with predator abundance (Figure 4) was mitigated, and this more complex scenario likely provided a better approximation of the realized impact of murre predation on juvenile Chinook salmon over our study period. Salmon survival rates decreased in years with the highest salmon diet fraction (e.g., 2004–2007). When common murre salmon diet fractions are high, predicted predation rates on salmon are predicted to be elevated even when the abundance of common murre is relatively low (e.g., 1996, Figure 5).
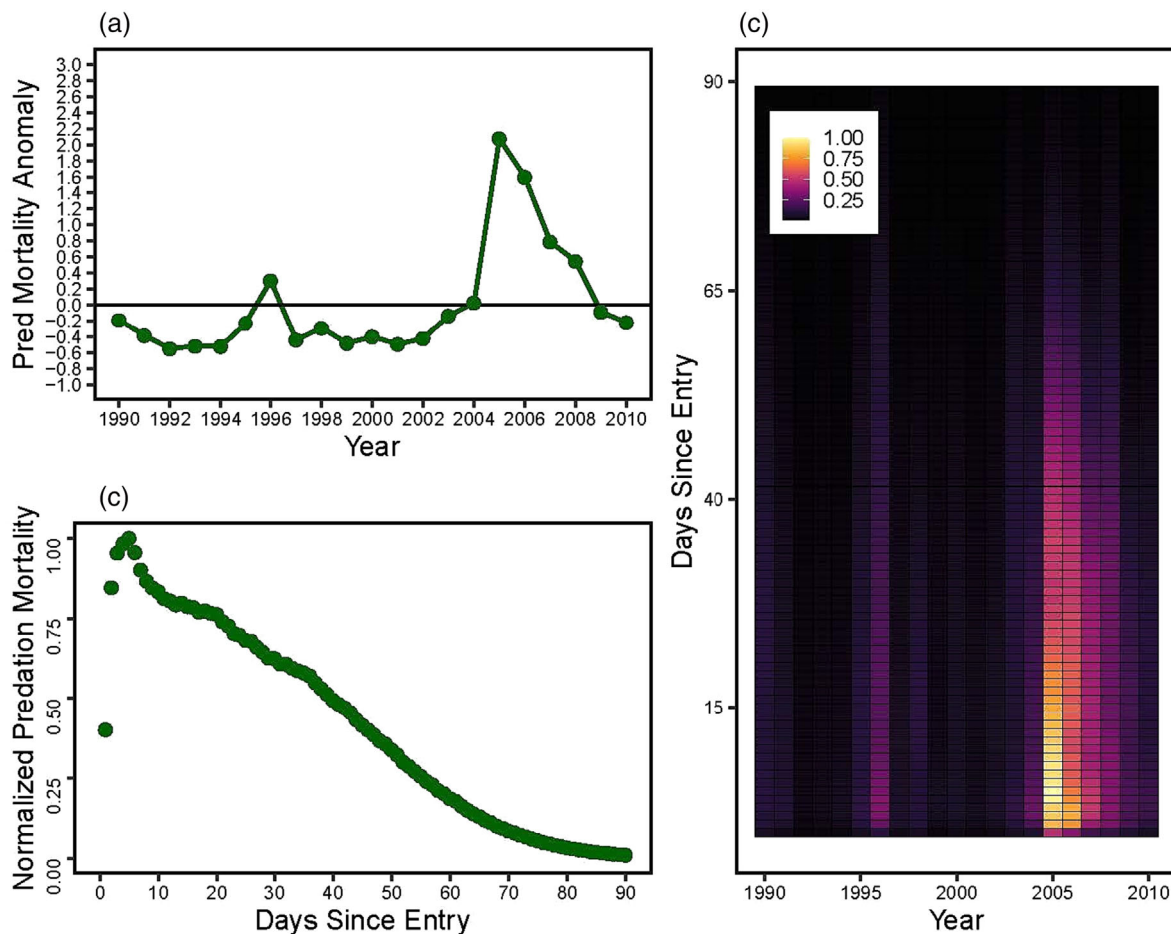

FIGURE 5 Simulated cumulative predation mortality from Scenario 4. (a) Anomaly from mean cumulative predation mortality during the first 90 days since entry. (b) Mean daily predation mortality rate averaged over all years as a function of days since entry and normalized so that the maximum value is one. (c) Normalized daily predation mortality rate by days since ocean entry for each year.
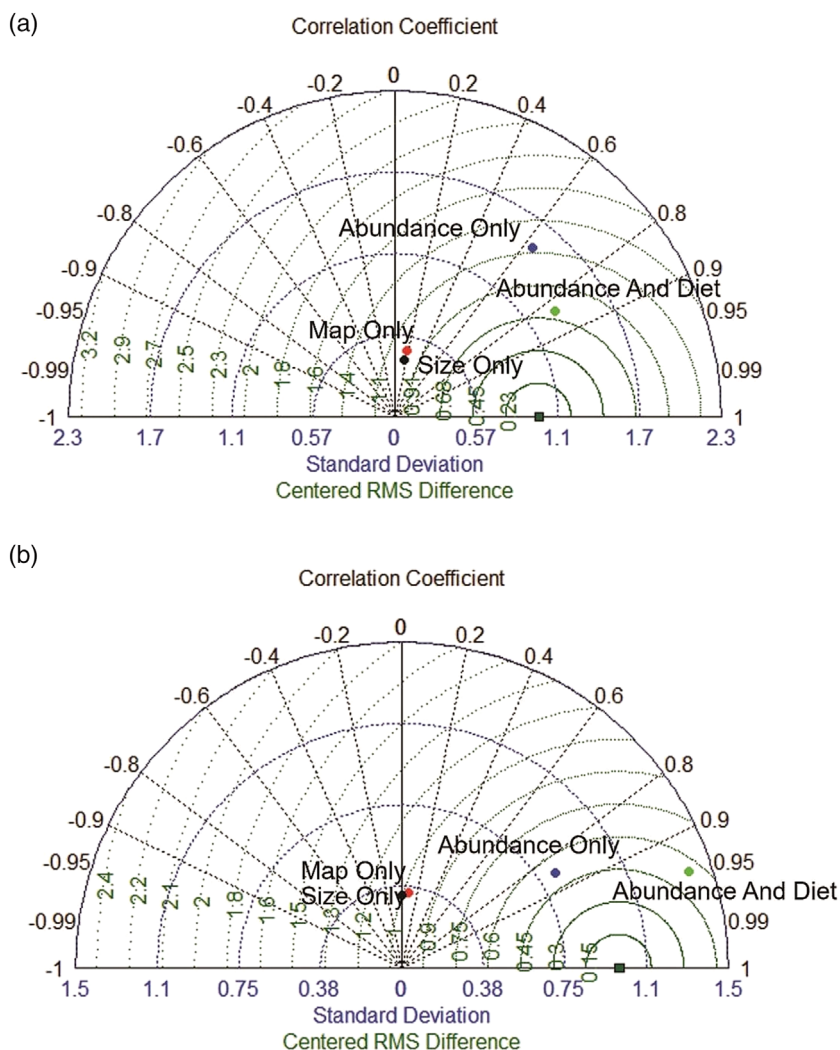
(a)

(b)

FIGURE 6 Taylor diagrams for (a) full time series and (b) post-2000 showing root-mean-squared differences (RMSD) normalized by observed standard deviation (green circles), modal-data correlation (azimuthal angle), and ratio of simulated to observed standard deviation (radial distance). Perfect model-data agreement coincides with the point (1, 1). Scenarios 1–4 are denoted in order of increasing complexity: (Scenario 1, black dot) size only (Scenario 2, red dot) size + map only (Scenario 3, blue dot) abundance + map (Scenario 4, green dot) size + map + abundance + diet.

Our results are not always in agreement with empirical estimates of smolt-to-adult survival of these cohorts from Henderson et al. (2019) or Kilduff et al. (2014), especially during years of overall high salmon survival accumulated across the first ocean year. Based on tag data, Henderson et al. (2019) and Kilduff et al. (2014) estimated salmon survival to be average in 1996 and well above average in 2000. Fiechter et al. (2015) used the 2000 cohort as an example of presumed high survival for examination of growth dynamics during early ocean residence. Our IBM simulations (Scenarios 1–4) predicted salmon survival to be low in 1996 but average in 2000, so our results do not fully align with these earlier studies (Figure 5). This example highlights an important potential difficulty in the comparison of early marine survival estimates to smolt-to-adult ratio estimates from hatchery release, which can be strongly influenced by the freshwater conditions experienced by smolts before they reach the ocean (Michel, 2019). Our IBM-predicted survivals are based on growth and predation during the first 90 days after ocean entry and thus need to be viewed in the context of survival during the first period at sea. The estimates from Kilduff et al. (2014) are based on coded-wire-tag recoveries that conflate survival variations from hatchery release to the end of first ocean winter, including the freshwater period. In fact, a closer examination of Henderson et al. (2019) shows that as the first-year survival estimate increases, variability around their statistical fit also increases; in this example, predicted values match observed values much better at lower survivals, indicating that poor ocean conditions impact the overall first-year survival in a significant manner but that during more favorable conditions, additional drivers must be considered. More directly, while the coastal ecosystem imparted its impacts on population survival during early ocean residency, the mortality of these cohorts accumulated across the first year of life may also have been related to freshwater conditions (Michel, 2019) or to events during a later period at sea (Beamish & Mahnken, 2001).

The statistical life-cycle model developed by Friedman et al. (2019) also predicted a significant negative impact of early marine predation on the 1996 cohort during its early ocean residency and a significant positive association of freshwater flow on the survival of the 2000 cohort while in freshwater. Michel (2019) supports low survivals for 2005 and 2006 related to unfavorable ocean conditions, as does Lindley et al. (2009). Our results also show higher predation and lower survival in these 2 years in Scenarios 3 and 4. In total, our findings

provide context for the sensitivity of salmon survival to the ocean environment, predation, and diet fraction as influenced by alternative prey and, ultimately, when considered additively within a full life cycle model (e.g., Friedman et al., 2019), can provide a mechanistic approach for estimating early marine juvenile salmon survival. Our results can also inform the potential outcomes on salmon survival from management strategies that directly or indirectly relate to predator abundance and forage availability at sea. The predator included here represents a central-place foraging seabird species, but the model could easily be extended to other predator types (e.g., migratory fish, marine mammals, or other sea bird predators).

4.2 | Impact of growth and predator overlap on survival

The function of predation mortality with respect to prey size over the range of the common murre gape indicates that more rapid growth leads to less predation mortality and therefore better early marine survival. In the simplest scenario without a predator spatial distribution, predation mortality decreases immediately with size (and age, as long as simulated individuals have positive growth rates). Overall survival in a scenario with uniform spatial overlap with a predator is, therefore, a direct result of growth and it is advantageous for a fish to grow out of the gape window of their potential predators as quickly as possible. Hence, larger size serves as a refuge from predation. Future work in the development of this IBM aims to expand the behavioral ability of simulated juveniles to escape predation in spatial refugia by adding predator avoidance behavior to the between grid-cell movements of the super-individuals.

During the breeding season, common murre are central place feeders, moving between breeding colonies on Southeast Farallon Island where their young are located and the GoF where they capture prey (Santora et al., 2014; Wells et al., 2017). When a fixed spatially varying seabird distribution is specified, juvenile salmon predation mortality increases to a peak a few days after ocean entry and then decreases with time, indicating that juvenile salmon experience increased predation mortalities early in their marine life in areas that overlap with higher concentrations of common murre.

4.3 | Predation mortality and model complexity

The question of variable inclusion is relevant from the simplest linear regression up to the most complex end-to-end modeling systems (Collie et al., 2016). Our ecosystem model couples highly detailed information about regional hydrodynamics and lower trophic level drivers with a simplified representation of predation to achieve a model that is able to match high and low survival years estimated from datasets derived from a coded wire tag survey and other age structured models for Chinook salmon in the CCS (Friedman et al., 2019; Henderson et al., 2019; Michel, 2019). The four predation scenarios considered here constitute an exercise in developing

modeling complexity. Our assumption is that adding more biophysical drivers results in a more realistic (and presumably adequate) representation of the dynamic system. This approach is consistent with that of determining a model of intermediate complexity (Collie et al., 2016; Plagányi et al. 2012), which can accurately represent the system (e.g., as observed in Wells et al., 2017, and Woodson et al., 2013), without overexplaining the variance or increasing parameter uncertainty. Our model results indicate that predator–prey dynamics of juvenile salmon and central-place foraging predators such as seabirds can be represented in this region through the inclusion of three key pieces of information: (1) the relationship between bottom-up drivers and juvenile growth out of a size-based vulnerability window, (2) predator distribution and relative population size, and (3) the predator diet percentage made up of juvenile salmon.

Comparing results of model predicted predation mortality and survival to previously published datasets of juvenile survival such as the coded wire tag data (Henderson et al., 2019) indicates that a size-based mortality model alone will not accurately represent the predation mortality in this area. Further, adding the predator spatial distribution component is not sufficient to represent the system as salmon predator population sizes increase. For example, juvenile survival in observational datasets is low from 2004 to 2007, but these are years when juveniles reached above-median sizes (approximately 133–137 mm, compared with a range of 120–142 mm over all years) during their early ocean entry period, so the addition of a predation (top-down) driver is necessary to match the observed low survivals.

Taylor diagrams for the full 21-year time series and the times series ranging only from 2000 to 2010 indicate that for both time periods, Scenarios 2 (map only), 3 (abundance), and 4 (abundance and diet) bring the model incrementally closer to the observations of the system, as correlation coefficients increase, ratio of standard deviations get closer to 1, and centered RMS difference decreases each time an additional piece of predator information is added (Figure 6). The most complex scenario (4) exhibits the best agreement with the observations (i.e., lowest normalized RMSD for both the full time period [1990–2010] and the period of higher predator abundance [2000–2010]). During the second half of the time series, when common murre breeding populations are high, the correlation of Scenario 4 predictions to the observed time series is very close to 1, indicating that while adding predation to the model is still useful during mid-to-low predation years, adding predator abundance and diet information to the model is especially crucial during high predation years and improves model performance under these conditions.

Scenario 4, which includes all three sets of information, is thus the best representation of the system when compared with known survival values and patterns. When checked against other observational datasets, this scenario is able to reproduce highs and lows in key years such as low survivals in 1996 and from 2005 to 2007 (Friedman et al., 2019; Michel, 2019) and high survivals in 1999–2000 as well as 2008–2010 (Friedman et al., 2019; Michel, 2019). We believe that this scenario is the most ecologically relevant as it captures survival dynamics related to both predator population sizes and the favorable ocean conditions.

4.4 | The need for synchronous recovery

Synchronous recovery, or the simultaneous recovery of predators and prey in an ecosystem, is both faster and more direct than sequential prey-first or predator-first recovery and has been suggested as a better way to meet both social and ecological ecosystem management goals (Samhouri et al., 2017). The central-place feeding predator and juvenile salmon prey interaction presented in this study supports the idea of synchronous recovery. When predator abundance values are introduced into the IBM, they quickly overwhelm environmental variability as a driver (Scenario 3). If alternative prey is unavailable, salmon survival rapidly decreases as predator numbers increase (Scenario 3). If alternative prey is available, as indicated in our study by proportional diet data, negative trends in survival are mitigated (Scenario 4), indicating a need for the synchronous recovery of forage prey as predator populations recover. Our results suggest that the recovery of predators without alternative prey numbers also rising leads to an unintended consequence on salmon survival, as the predators will turn to salmon instead of alternative forage, a real-world situation observed by Wells et al. (2017). Therefore, any ecosystem-based strategies to be evaluated and implemented should include consideration of both predator variability and trends along with measures to protect their forage, which in the California Current includes coastal pelagic species, crab larvae, squid, krill, juvenile rockfish, and smelt. Ecosystem-based modeling frameworks aiming to aid the survival of salmon need to protect forage, providing alternative prey to predators of juvenile salmon.

4.5 | Spatial aspects of survival

Timing, strength, and duration of upwelling winds, wind stress curl, and the resulting habitat availability and spatial heterogeneity in the seascape are critical aspects of this coastal ecosystem having consequences on the availability of forage, seabird productivity and behavior, and the growth, condition, and survival of juvenile salmon (Sabal et al., 2020; Santora, Schroeder, et al., 2021; Warzybok et al., 2018; Wells et al., 2008, 2017). Our modeling results support the idea that the probability of survival has a spatially explicit component off Central California, which is consistent with previous findings that southern areas of the GoF have greater potential for variability in the growth and survival of juvenile salmon than northern regions, despite the larger populations of juvenile salmon found in northern GoF (Hassrick et al., 2016; Henderson et al., 2019). The southern region of high mortality we identified, a persistent hotspot at Pioneer Canyon (Santora et al., 2018), has also been shown to have high feeding aggregations of common murre in response to anchovy (Santora et al., 2012; Wells et al., 2017), especially during periods of suboptimal upwelling dynamics when the upwelling shadow south of Point Reyes has less retained prey (Wing et al., 1998). This feeding aggregation area is captured by our predator distribution map (Figure 1b, southern hotspot), and when included in the IBM, we can identify the impact of feeding aggregations on spatial predation mortality patterns (Figure 2d vs. 2e). The increased availability of forage in the southern GoF due to higher productivity as well as the increased size of juveniles reaching this area is likely mitigating the impact of this common murre feeding aggregation on juvenile salmon survival (Hassrick et al., 2016; Henderson et al., 2019). Specifically, due to the interactions between forage, common murre, and juvenile salmon in the southern GoF, the growth of salmon there is correlated to population survival. By including explicit top-down predator impacts on juvenile survival and a mitigation factor in the form of the alternate prey in the diet of predators (Fiechter et al., 2015; Henderson et al., 2019), the updated version of the IBM can capture potential mechanisms leading to results documented in previous studies in this region.

4.6 | Moving the IBM into predictive space

Scenario 4 shows that including information about diet modulates the effect of predator abundance on salmon survival (i.e., Scenario 3), which suggests an important role for the availability of alternative prey species. In the California Current Ecosystem, predation risk for juvenile salmon by seabirds has been shown to be related to other prey species that were collocated with salmon and seabirds (Wells et al., 2017). Future work on this project seeks to represent diet composition as an emergent property of the IBM by predicting seabird and alternative forage distributions from environmental data. Common murre in the GoF have been shown to feed more heavily on salmon in years when juvenile rockfish are scarce and Northern anchovy are relatively abundant in nearshore areas of the GoF, where they are collocated with juvenile salmon. The abundance of forage fish in the region has also been linked to the sea-state regime present in the GoF (Santora et al., 2014; Wells et al., 2017). If the distribution and relative abundance of predators and alternative forage species can be predicted from environmental conditions, the amount that a predator feeds on salmon versus other prey can become an emergent property of the model instead of an input parameter. While the current parameterization of the IBM can represent past juvenile survival patterns, we are working to move the IBM into predictive space to assess alternative mitigation strategies for years of unfavorable growth conditions. If successful, the model could provide early warning of poor salmon recruitment to fishery managers.

CONFLICT OF INTEREST STATEMENT

The authors have declared no conflict of interest.

DATA AVAILABILITY STATEMENT

RREAS data are available at https://coastwatch.pfeg.noaa.gov/erddap/tabledap/FED_Rockfish_Catch.html The model output from scenarios used here will be deposited to our repository on Dryad with a reference DOI of doi:10.5061/dryad.8sf7m0cvs.

ORCID

Kelly Vasbinder https://orcid.org/0009-0006-0061-5592

REFERENCES

Anderson, J. J. (2019). Survival of prey growing through gape-limited and apex predators. *BioRxiv*, June, 686964. https://doi.org/10.1101/686964

Beamish, R. J., & Mahnken, C. (2001). A critical size and period hypothesis to explain natural regulation of salmon abundance and the linkage to climate and climate change. *Progress in Oceanography*, 49(1–4), 423–437. https://doi.org/10.1016/S0079-6611(01)00034-9

Beamish, R. J., Mahnken, C., & Neville, C. M. (2004). Evidence that reduced early marine growth is associated with lower marine survival of coho salmon. *Transactions of the American Fisheries Society*, 133(1), 26–33. https://doi.org/10.1577/T03-028

Bolar, K. (2019). The STATS package. Interactive document for working with basic statistical analysis. Kartikeya Bolar, Karnataka, India. https://cran.r-project.org/web/packages/STAT/STAT.pdf

Brandes, P. L., & McLain, J. S. (2001). Juvenile Chinook salmon abundance, distribution, and survival in the Sacramento–San Joaquin Estuary. In R. L. Brown (Ed.), *Contributions to the biology of Central Valley salmonids, vol 2. Fish Bulletin No. 179* (pp. 39–138). Sacramento (CA).

Brinton, E. (1962). The distribution of Pacific euphausiids. University of California Press, 225. n.d. *Variable factors affecting the apparent range and estimated concentration of euphausiids in the North Pacific*, 35.

Collie, J. S., Botsford, L. W., Hastings, A., Kaplan, I. C., Largier, J. L., Livingston, P. A., Plagányi, É., Rose, K. A., Wells, B. K., & Werner, F. E. (2016). Ecosystem models for fisheries management: Finding the sweet spot. *Fish and Fisheries*, 17(1), 101–125. https://doi.org/10.1111/faf.12093

Daly, E. A., & Brodeur, R. D. (2015). Warming ocean conditions relate to increased trophic requirements of threatened and endangered salmon. *PLoS ONE*, 10(12), e0144066. https://doi.org/10.1371/journal.pone.0144066

Duffy, E. J., & Beauchamp, D. A. (2011). Rapid growth in the early marine period improves the marine survival of Chinook salmon (*Oncorhynchus tshawytscha*) in Puget Sound, Washington. *Canadian Journal of Fisheries and Aquatic Sciences*, 68(2), 232–240. https://doi.org/10.1139/F10-144

Fiechter, J., Buil, M. P., Jacox, M. G., Alexander, M. A., & Rose, K. A. (2021). Projected shifts in 21st century sardine distribution and catch in the California current. *Frontiers in Marine Science*, 8, 874.

Fiechter, J., Edwards, C. A., & Moore, A. M. (2018). Wind, circulation, and topographic effects on alongshore phytoplankton variability in the California current. *Geophysical Research Letters*, 45, 3238–3245. https://doi.org/10.1002/2017GL076839

Fiechter, J., Huff, D. D., Martin, B. T., Jackson, D. W., Edwards, C. A., Rose, K. A., Curchitser, E. N., Hedstrom, K. S., Lindley, S. T., & Wells, B. K. (2015). Environmental conditions impacting juvenile Chinook salmon growth off Central California: An ecosystem model analysis: Environmental impacts on salmon growth. *Geophysical Research Letters*, 42(8), 2910–2917. https://doi.org/10.1002/2015GL063046

Fiechter, J., Santora, J. A., Chavez, F., Northcott, D., & Messié, M. (2020). Krill hotspot formation and phenology in the California current ecosystem. *Geophysical Research Letters*, 47, e2020GL088039. https://doi.org/10.1029/2020GL088039

Friedman, W. R., Martin, B. T., Wells, B. K., Warzybok, P., Michel, C. J., Danner, E. M., & Lindley, S. T. (2019). Modeling composite effects of marine and freshwater processes on migratory species. *Ecosphere*, 10(7), e02743. https://doi.org/10.1002/ecs2.2743

Graham, W. M., Field, J. G., & Potts, D. C. (1992). Persistent upwelling shadows and their influence on zooplankton distributions. *Marine Biology*, 114(4), 561–570. https://doi.org/10.1007/BF00357253

Graham, W. M., & Largier, J. L. (1997). Upwelling shadows as nearshore retention sites: The example of northern Monterey Bay. *Continental Shelf Research*, 17(5), 509–532. https://doi.org/10.1016/S0278-4343(96)00045-3

Groot, C., & Margulis, L. (1991). *Pacific salmon life histories*. University of British Columbia Press. 564pp.

Hassrick, J. L., Henderson, M. J., Huff, D. D., Sydeman, W. J., Sabal, M. C., Harding, J. A., Ammann, A. J., Crandall, E. D., Bjorkstedt, E. P., Garza, J. C., & Hayes, S. A. (2016). Early ocean distribution of juvenile Chinook salmon in an upwelling ecosystem. *Fisheries Oceanography*, 25, 133–146. https://doi.org/10.1111/fog.12141

Healey, M. C. (1991). Diets and feeding rates of juvenile pink, chum, and sockeye salmon in Hecate Strait, British Columbia. *Transactions of the American Fisheries Society*, 120(3), 303–318. https://doi.org/10.1577/1548-8659(1991)120<0303:DAFROJ>2.3.CO;2

Henderson, M., Fiechter, J., Huff, D. D., & Wells, B. K. (2019). Spatial variability in ocean-mediated growth potential is linked to Chinook salmon survival. *Fisheries Oceanography*, 28(3), 334–344. https://doi.org/10.1111/fog.12415

Hjort, J. (1914). *Fluctuations in the great fisheries of northern Europe viewed in the light of biological research*. ICES.

Jager, T., Martin, B. T., & Zimmer, E. I. (2013). DEBkiss or the quest for the simplest generic model of animal life history. *Journal of Theoretical Biology*, 328, 9–18. https://doi.org/10.1016/j.jtbi.2013.03.011

Kilduff, D. P., Botsford, L. W., & Teo, S. L. H. (2014). Spatial and temporal covariability in early ocean survival of Chinook salmon (*Oncorhynchus tshawytscha*) along the west coast of North America. *ICES Journal of Marine Science*, 71(7), 1671–1682. https://doi.org/10.1093/icesjms/fsu031

Kishi, M. J., Kashiwai, M., Ware, D. M., Megrey, B. A., Eslinger, D. L., Werner, F. E., Noguchi-Aita, M., Azumaya, T., Fuji, M., & Hashimoto, S. (2007). NEMURO—A lower trophic level model for the North Pacific marine ecosystem. *Ecological Modelling*, 202(1–2), 12–25. https://doi.org/10.1016/j.ecolmodel.2006.08.021

Largier, J. L., Lawrence, C. A., Roughan, M., Kaplan, D. M., Dever, E. P., Dorman, C. E., Kudela, R. M., Bollens, S. M., Wilkerson, F. P., Dugdale, R. C., Botsford, L. W., Garfield, N., Kuebel Cervantes, B., & Koračin, D. (2006). WEST: A northern California study of the role of wind-driven transport in the productivity of coastal plankton communities. *Deep Sea Research Part II: Topical Studies in Oceanography*, 53(25–26), 2833–2849. https://doi.org/10.1016/j.dsr2.2006.08.018

Lindley, S. T., Grimes, C. B., Mohr, M. S., Peterson, W., Stein, J., Anderson, J. T., Botsford, L. W., Bottom, D. L., Busack, C. A., Collier, T. K., Ferguson, J., Garza, J. C. Grover, A. M., Hankin, D. G., Kope, R. G., Lawson, P. W., Low, A., MacFarlane, R. B., Moore, K., … Williams T.H. (2009). What caused the Sacramento River Fall Chinook stock collapse? *NOAA Technical Memorandum NMFS 447*. 125 p.

MacFarlane, R. B. (2010). Energy dynamics and growth of Chinook salmon (*Oncorhynchus tshawytscha*) from the Central Valley of California during the estuarine phase and first ocean year. Edited by Marc Trudel. *Canadian Journal of Fisheries and Aquatic Sciences*, 67(10), 1549–1565. https://doi.org/10.1139/F10-080

MacFarlane, R. B., & Norton, E. C. (2002). Physiological ecology of juvenile Chinook salmon (*Oncorhynchus tshawytscha*) at the southern end of their distribution, the San Francisco Estuary and Gulf of the Farallones, California. *Fish. Bull. (Wasington, D.C.)*, 100, 244, 257.

Michel, C. J. (2019). Decoupling outmigration from marine survival indicates outsized influence of streamflow on cohort success for California's Chinook salmon populations. *Canadian Journal of Fisheries and Aquatic Sciences*, 76, 1398–1410. https://doi.org/10.1139/cjfas-2018-0140

Myers, J. M., Kope, R. G., Bryant, G. J., Teel, D., Lierheimer, L. J., Wainwright, T. C., Grant, S. W., Waknitz, W. F., Neely, K., Lindley, S. T., & Waples, R. S. (1998). Status review of Chinook salmon from Washington, Idaho, Oregon, and California. US Department of Commerce, National Marine Fisheries Service, NOAA Technical Memorandum NMFS NWFSC-35.

Nelson, G. A. (2019). Bias in common catch-curve methods applied to age frequency data from fish surveys. Edited by Stan Kotwicki. *ICES Journal of Marine Science*, 76(7), 2090–2101. https://doi.org/10.1093/icesjms/fsz085

Neveu, E., Moore, A. M., Edwards, C. A., Fiechter, J., Drake, P., Jacox, M. G., & Nuss, E. (2016). An historical analysis of the California current using ROMS 4D-Var: System configuration and diagnostics. *Ocean Modelling*, 99, 133–151. https://doi.org/10.1016/j.ocemod.2015.11.012

Pearcy, W. G. (1992). *Ocean ecology of North Pacific salmonids*. University of Washington Sea Grant.

Plagányi, E., Punt, A. E., Hillary, R., Morello, E. B., Thébaud, O., Hutton, T., Pillans, R. D., Thorson, J. T., Fulton, E. A., Smith, A. D., Smith, F., Bayliss, P., Haywood, M., Lyne, V., & Rothlisberg, P. C. (2014). Multispecies fisheries management and conservation: Tactical applications using models of intermediate complexity. *Fish and Fisheries*, 15. n/a-n/a, 1–22. https://doi.org/10.1111/j.1467-2979.2012.00488.x

Punt, A. E., & Butterworth, D. S. (1995). The effects of future consumption by the cape fur seal on catches and catch rates of the cape hakes. 4. Modelling the biological interaction between cape fur seals *Arctocephalus pusillus pusillus* and the cape hakes *Merluccius capensis* and *M. paradoxus*. *South African Journal of Marine Science*, 16, 255–285. https://doi.org/10.2989/025776195784156494

Sabal, M. C., Hazen, E. L., Bograd, S. J., MacFarlane, R. B., Schroeder, I. D., Hayes, S. A., Harding, J. A., Scales, K. L., Miller, P. I., Ammann, A. J., & Wells, B. K. (2020). California current seascape influences juvenile salmon foraging ecology at multiple scales. *Marine Ecology Progress Series*, 634(January), 159–173. https://doi.org/10.3354/meps13185

Samhouri, J., Stier, A., Hennessey, S., Novak, M., Halpern, B., & Levin, P. (2017). Rapid and direct recoveries of predators and prey through synchronized ecosystem management. *Nature Ecology and Evolution*, 1, 0068. https://doi.org/10.1038/s41559-016-0068

Santora, J. A., Field, J. C., Schroeder, I. D., Sakuma, K. M., Wells, B. K., & Sydeman, W. J. (2012). Spatial ecology of krill, micronekton and top predators in the Central California current: Implications for defining ecologically important areas. *Progress in Oceanography*, 106-(November), 154–174. https://doi.org/10.1016/j.pocean.2012.08.005

Santora, J. A., Mantua, N. J., Schroeder, I. D., Field, J. C., Hazen, E. L., Bograd, S. J., Sydeman, W. J., Wells, B. K., Calambokidis, J., Saez, L., & Lawson, D. (2020). Habitat compression and ecosystem shifts as potential links between marine heatwave and record whale entanglements. *Nature Communications*, 11(1), 536. https://doi.org/10.1038/s41467-019-14215-w

Santora, J. A., Rogers, T. L., Cimino, M. A., Sakuma, K. M., Hanson, K. D., Dick, E. J., Jahncke, J., Warzybok, P., & Field, J. C. (2021). Diverse

integrated ecosystem approach overcomes pandemic-related fisheries monitoring challenges. *Nature Communications*, 12, 6492. https://doi.org/10.1038/s41467-021-26484-5

Santora, J. A., Schroeder, I. D., Bograd, S. J., Chavez, F. P., Cimino, M. A., Fiechter, J., Hazen, E. L., Kavanaugh, M. T., Messié, M., Miller, R. R., & Sakuma, K. M. (2021). Pelagic biodiversity, ecosystem function, and services. *Oceanography*, 34(2), 16–37. https://doi.org/10.5670/oceanog.2021.212

Santora, J. A., Schroeder, I. D., Field, J. C., Wells, B. K., & Sydeman, W. J. (2014). Spatio-temporal dynamics of ocean conditions and forage taxa reveal regional structuring of seabird–prey relationships. *Ecological Applications*, 24(7), 1730–1747. https://doi.org/10.1890/13-1605.1

Santora, J. A., Zeno, R., Dorman, J. G., & Sydeman, W. J. (2018). Submarine canyons represent an essential habitat network for krill hotspots in a Large Marine Ecosystem. *Scientific Reports*, 8(1). https://doi.org/10.1038/s41598-018-25742-9

Taylor, K. E. (2001). Summarizing multiple aspects of model performance in a single diagram. *Journal of Geophysical Research*, 106, 7183–7192 (also see PCMDI Report 55. http://wwwpcmdi.llnl.gov/publications/ab55.html, https://doi.org/10.1029/2000JD900719

Trudel, M., Middleton, D. W., Tucker, S., Thiess, M. E., Morris, J. F. T., Candy, J. R., Mazumder, A., & Beacham, T. D. (2012). Estimating winter mortality in juvenile Marble River Chinook salmon. NPAFC Doc. 1426. 14 pp. Available at http://www.npafc.org

Trudel, M. A., Thiess, M. E., Bucher, C. Y., Farley, E. V., MacFarlane, R. B., Casillas, E. D., Fisher, J. O., Morris, J. F., Murphy, J. M., & Welch, D. W. (2007). Regional variation in the marine growth and energy accumulation of juvenile Chinook Salmon and Coho salmon along the West Coast of North America. In C. B. Grimes, R. D. Brodeur, L. J. Haldorson, & S. M. McKinnell (Eds.), *Ecology of juvenile salmon in the Northeast Pacific Ocean: Regional comparisons* (pp. 205–232). American Fisheries Society. Symposium 57, Bethesda, Maryland.

Walters, C. J., & Juanes, F. (1993). Recruitment limitation as a consequence of natural selection for use of restricted feeding habitats and predation risk taking by juvenile fishes. *Canadian Journal of Fisheries and Aquatic Sciences*, 50(10), 2058–2070. https://doi.org/10.1139/f93-229

Wang, S. C., & Novack-Gottshall, P. (2016). Package 'KScorrect' title Lilliefors-corrected Kolmogorov–Smirnoff goodness-of-fit tests.

Warzybok, P., Santora, J. A., Ainley, D. G., Bradley, R. W., Field, J. C., Capitolo, P. J., Carle, R. D., Elliott, M., Beck, J. N., McChesney, G. J., & Hester, M. M. (2018). Prey switching and consumption by seabirds in the Central California current upwelling ecosystem: Implications for forage fish management. *Journal of Marine Systems*, 185, 25–39. https://doi.org/10.1016/j.jmarsys.2018.04.009

Watkins, K. S., & Rose, K. A. (2013). Evaluating the performance of individual-based animal movement models in novel environments. *Ecological Modelling*, 250, 214–234. https://doi.org/10.1016/j.ecolmodel.2012.11.011

Weitkamp, L. A. (2010). Marine distributions of Chinook salmon from the west coast of North America determined by coded wire tag recoveries. *Transactions of the American Fisheries Society*, 139(1), 147–170. https://doi.org/10.1577/T08-225.1

Wells, B., Santora, J., Bizzarro, J., Billings, A., Brodeur, R., Daly, E., Field, J., Richerson, K., & Thorson, J. (2023). Trophoscapes of predatory fish reveal biogeographic structuring of spatial dietary overlap and inform fisheries bycatch patterns. *Marine Ecology Progress Series*, SPF2. https://doi.org/10.3354/meps14319

Wells, B. K., Field, J. C., Thayer, J. A., Grimes, C. B., Bograd, S. J., Sydeman, W. J., Schwing, F. B., & Hewitt, R. (2008). Untangling the relationships among climate, prey and top predators in an ocean ecosystem. *Marine Ecology Progress Series*, 364, 15–29. https://doi.org/10.3354/meps07486

Wells, B. K., Huff, D. D., Burke, B. J., Brodeur, R. D., Santora, J. A., Field, J. C., Richerson, K., Mantua, N. J., Fresh, K. L., McClure, M. M., &

Satterthwaite, W. H. (2020). Implementing ecosystem-based management principles in the design of a salmon ocean ecology program. *Frontiers in Marine Science*, 7, 342.

Wells, B. K., Santora, J. A., Field, J. C., MacFarlane, R. B., Marinovic, B. B., & Sydeman, W. J. (2012). Population dynamics of Chinook salmon *Oncorhynchus tshawytscha* relative to prey availability in the Central California coastal region. *Marine Ecology Progress Series*, 457(June), 125–137. https://doi.org/10.3354/meps09727

Wells, B. K., Santora, J. A., Henderson, M. A., Warzybok, P., Jahncke, J., Bradley, R. W., Huff, D. D., Schroeder, I. D., Nelson, P., Field, J. C., & Ainley, D. G. (2017). Environmental conditions and prey-switching by a seabird predator impact juvenile Salmon survival. *Journal of Marine Systems*, 174, 54–63. https://doi.org/10.1016/j.jmarsys.2017.05.008

Wells, B. K., Santora, J. A., Schroeder, I. D., Mantua, N., Sydeman, W. J., Huff, D. H., & Field, J. C. (2016). Marine ecosystem perspectives on Chinook salmon recruitment: A synthesis of empirical and modeling studies from a California upwelling system. *Marine Ecology Progress Series*, 552(June), 271–284. https://doi.org/10.3354/meps11757

Willette, T. M. (2001). Foraging behaviour of juvenile pink salmon (*Oncorhynchus gorbuscha*) and size-dependent predation risk. *Fisheries Oceanography*, 10(s1), 110–131. https://doi.org/10.1046/j.1054-6006.2001.00042.x

Willette, T. M., Cooney, R. T., Patrick, V., Mason, D. M., Thomas, G. L., & Scheel, D. (2001). Ecological processes influencing mortality of juvenile pink salmon (*Oncorhynchus gorbuscha*) in Prince William Sound, Alaska. *Fisheries Oceanography*, 10(s1), 14–41. https://doi.org/10.1046/j.1054-6006.2001.00043.x

William, C. (1969). Rational Chebyshev approximations for the error function. *Mathematics of Computation*, 23, 631–637.

William, C. (1993). Algorithm 715: SPECFUN—A portable FORTRAN package of special function routines and test drivers. *ACM Transactions on Mathematical Software*, 19(1), 22–32. https://doi.org/10.1145/151271.151273

Wing, S. R., Botsford, L. W., Ralston, S. V., & Largier, J. L. (1998). Meroplanktonic distribution and circulation in a coastal retention zone of the northern California upwelling system. *Limnology and Oceanography*, 43(7), 1710–1721. https://doi.org/10.4319/lo.1998.43.7.1710

Woodson, C. B., & Litvin, S. Y. (2015). Ocean fronts drive marine fishery production and biogeochemical cycling. *Proceedings of the National Academy of Sciences U S A*, 112(6), 1710–1715. https://doi.org/10.1073/pnas.1417143112

Woodson, L. E., Wells, B. K., Weber, P. K., MacFarlane, R. B., Whitman, G. E., & Johnson, R. C. (2013). Size, growth, and origin-dependent mortality of juvenile Chinook salmon *Oncorhynchus tshawytscha* during early ocean residence. *Marine Ecology Progress Series*, 487(July), 163–175. https://doi.org/10.3354/meps10353